electronics

MDPI

Article

Accessible and Inexpensive Parameter Testing Platform for Adhesive Removal in Mechanical Exfoliation Procedures

Anthony Gasbarro [1,2,*], Yong-Sung D. Masuda [2], Richard C. Ordonez [1], Jeffrey A. Weldon [2] and Victor M. Lubecke [2]

[1] Graphene Microfluidic Laboratory, Naval Information Warfare Center Pacific, Pearl City, HI 96782, USA; richard.c.ordonez.civ@us.navy.mil
[2] Department of Electrical and Computer Engineering, University of Hawai'i at Mānoa, Honolulu, HI 96822, USA; ydmasuda@hawaii.edu (Y.-S.D.M.); jaweldon@hawaii.edu (J.A.W.); lubecke@hawaii.edu (V.M.L.)
* Correspondence: agasbarr@hawaii.edu

Abstract: Mechanical exfoliation of two-dimensional (2D) materials using adhesive tape is a widely used method for producing high-quality single-layer graphene flakes. However, this technique is time-consuming, with low yields and inconsistent results due to process variations and human error. This paper introduces a modular system designed to rigorously test and optimize the conditions for 2D material deposition, with a focus on graphene. The system is adaptable to a range of inexpensive, commercially available linear stages and stepper motors, providing precise, independent control over key parameters such as peel speed and angle—both of which are critical in deposition yields. Tests confirmed the system's accuracy within ±0.7% relative speed error across a range of speeds (1 µm/s to 5000 µm/s) and peel angle control from 0° to 120°. Additionally, the system automates control of the key factors at the most demanding step of the exfoliation process while being affordable and easily assembled, making it accessible for laboratories and educational institutions to explore the optimal conditions for scaling 2D material production. This system offers the capability to gain critical insights into the exfoliation process, driving improved yields and scalability, which are essential for fabricating highly specialized devices that rely on 2D materials.

Keywords: graphene; mechanical exfoliation; 2D materials; parameter testing

Academic Editor: Yahya M. Meziani

Received: 28 December 2024
Revised: 22 January 2025
Accepted: 27 January 2025
Published: 28 January 2025

Citation: Gasbarro, A.; Masuda, Y.-S.D.; Ordonez, R.C.; Weldon, J.A.; Lubecke, V.M. Accessible and Inexpensive Parameter Testing Platform for Adhesive Removal in Mechanical Exfoliation Procedures. *Electronics* **2025**, *14*, 533. https://doi.org/10.3390/electronics14030533

1. Introduction

Graphene was first identified in Novoselov and Geim's seminal 2004 publication using a mechanical exfoliation method commonly known as the "Scotch-Tape technique" [1]. Over the past two decades, significant advancements have been made in leveraging the novel capabilities of 2D materials through the creation of multi-layered material stacks called van der Waals heterostructures [2]. These heterostructures have shown promise as a new source of unique properties in highly sensitive applications such as superconductors for quantum computing and high-precision RF sensors [3–6]. Producing high-quality, single-layer, single-grain flakes of material is essential for these fine-tuned applications.

The widely used "Scotch-Tape technique" has seen little improvement despite its long-standing use. While still regarded as reliable, this procedure is labor-intensive, yields low output, and produces small flakes due to manual execution. Several studies have theoretically analyzed factors that could optimize material deposition using this method, while other research has offered automated solutions to streamline the process [7–10]. However, there is a gap in fundamental research on the practical analysis of the isolated

individual factors that affect flake deposition onto substrates. The traditional techniques for automating mechanical exfoliation systems do not factor in the normalization of peel speeds across different angles and are often expensive, complex, and require specialized components, limiting their accessibility to researchers and educators. Addressing this gap is crucial to enabling mass production of these materials and harnessing their potential on a larger scale.

In this publication, an instrument and methodology are introduced that offer the ability to test and isolate specific conditions that have a large effect on yield, as well as automate control specific parameters during one of the most time-consuming portions of the procedure. The system is assembled from readily available, low-cost, off-the-shelf parts and open-source software. It can precisely control peeling speeds and calculate corrections for variations in accuracy that would normally be introduced when testing substrates at different angles. This instrument allows for slower peel speeds over a significantly extended completion time, which would be impractical to achieve using manual techniques.

2. Materials and Methods

2.1. Background

Mechanical exfoliation using adhesive tape is a simple, straightforward technique, with fewer variables to control compared to alternative methods. While alternative methods can offer scalability or more control of key parameters, the adverse effects they introduce can compromise the quality of the resulting material, making mechanical exfoliation still preferable for certain sensitive applications requiring pristine, high-quality flakes [11]. The liquid phase exfoliation technique often introduces defects and contaminants through liquid contact. The chemical vapor deposition (CVD) of graphene allows for the relatively precise control of the parameters involved in crystalline growth during the deposition of graphene, but other publications have shown CVD to produce grain boundaries which degrade the electrochemical properties of the material [12–14]. Although recent advances in this area with other materials, such as WSe_2 and MoS_2, suggest the CVD method may become a compelling alternative for graphene in the future [15].

The mechanical exfoliation procedure uses a target SiO_2 wafer substrate, pre-cleaned using methods such as solvent washes, sonication, and O_2 plasma cleaning. The mechanical exfoliation portion of the procedure begins with bulk crystal of highly ordered pyrolytic graphite (HOPG) or other intended material and a piece of ordinary commercially available Scotch® (3M, Maplewood, MN, USA) brand adhesive tape. The adhesive tape is brought into contact with the HOPG bulk material then removed, cleaving off several flakes of the stacked layers of 2D graphene material with it. The flake-coated area of the adhesive is brought into contact with an unused portion of the tape then peeled apart. This is repeated multiple times to cleave these material stacks to a reduced amount of stacked layers. The material covered tape is then applied to the target SiO_2 wafer's surface and pressed down. The graphite layers applied to the surface of the substrate and are attracted to the SiO_2 wafer through van der Waals forces. The resulting stack is then heat annealed on a hotplate at 100 °C for ~2 min. Annealing facilitates the migration of gas adsorbates trapped between the SiO_2 surface and graphene flake, promoting larger areas of surface contact and enhancing adhesion [8,16,17].

The tape is peeled from the substrate, with the optimal outcome being that the van der Waals forces between the graphene layer and the SiO_2 substrate overcome the stacking forces between the graphene layers, as shown in Figure 1. A successful removal leaves only a single-layer graphene flake of material behind with a maximal surface area sample to fabricate into a device.

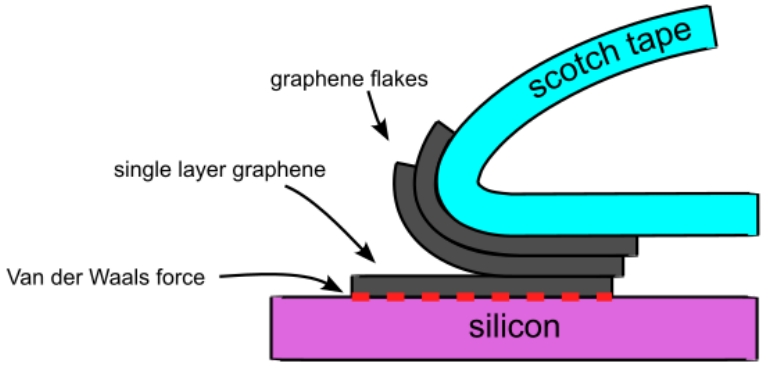

Figure 1. A diagram profile view illustrating the mechanics behind deposition of single-layer graphene with exaggerated flakes for clarity.

Published theoretical exploration has suggested that the peeling angle and speed are the most important aspects of the peeling process and suggest that adhesive forces scale quadratically with peel velocity. This implies that lower peel speeds are more effective for maintaining adhesion between a single-layer flake and the target substrate [8]. The tape peeling step of the procedure can be considered the most critical moment of single-layer material deposition. This step is typically performed by the hand of a technician, resulting in significant variability between deposition runs. The outcome is highly dependent on the technician's expertise, making it challenging to achieve consistent, precise, and repeatable results. The speed and angle of the peel are quantifiable metrics that can be measured and enforced rather than being subject to unpredictability of human error. Very few articles offering the specifications for automated systems for the mechanical exfoliation deposition step have been published, and those that have been preprinted or published each require individual expensive and custom machined components (many in excess of USD 2000 each), do not address the normalization of peel speeds across different angles or combine many variables at once, making quantitative study of individual factors difficult [9,10,18]. The system presented in this publication is not designed to simply automate the production of high-quality flakes; it allows for the isolated analysis of the factors that improve the deposition of high-quality flakes and provide a low-cost, accessible solution for researchers and educators.

2.2. System Description

Early efforts to automate the adhesive removal step focused on achieving a controlled, slow peel speed over extended periods. These attempts were tested using a modified 3D printer axis and a basic motor controller governed by revolutions per minute (RPM). The current system is a custom design tailored for mechanical exfoliation, incorporating software that accurately converts user-defined peel speed into precise motor movements. The control system, powered by an Arduino and programmed in C++, receives serial commands via a USB connection for starting, stopping, homing, and calculating the peel velocity at specific angles.

The linear pull system features a rigid frame and a stable foundation to minimize mechanical errors during testing. It utilizes a CNC double linear guide rail and a NEMA-57 stepper motor, which provides sufficient torque to overcome adhesive resistance and maintain consistent peel speeds without velocity fluctuations. The mounting surfaces and tabletop adapters were designed using Autodesk Fusion 360 v2.0.20754 CAD software and 3D printed for easy customization. These modular components allow for simple replacement and modification. The system can also be disassembled and reassembled for storage or transport.

A primary design objective was the use of widely available, low-cost materials to facilitate broader adoption and further development by other researchers. The total cost of the components required for this setup can be purchased for under USD 400 (and under USD 600 when adding the cost of a 3D printer). A model of the system is shown in Figure 2 and a summary of the expenses is presented in Table 1.

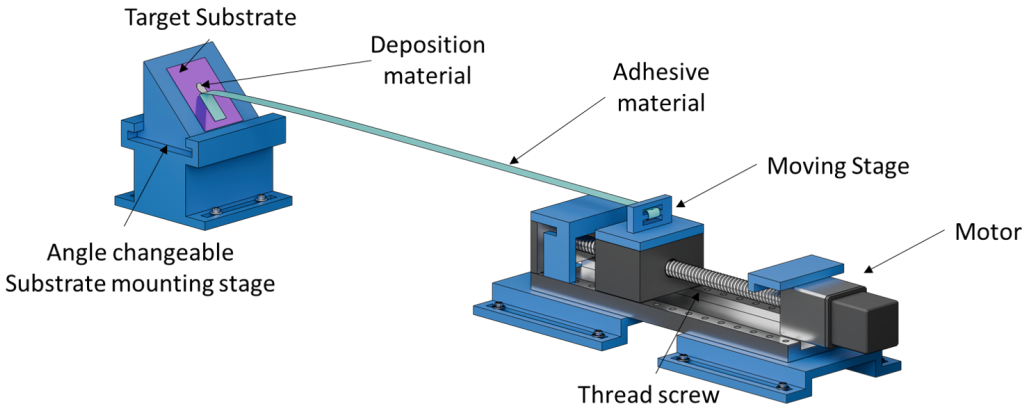

Figure 2. CAD model of the assembled system in operation, with 3D-printed components shown in blue.

Table 1. Breakdown of Components.

Component	Description	Distributor (Accessed on 10 June 2024)	Price (US$)
Motor Control System	Arduino UNO R3	Amazon	$13.59
Arduino expansion board	CNC shield expansion	Amazon	$7.99
Stepper motor driver	TMC2209 V1.3	Amazon	$29.99
Linear actuator and motor	600 mm Linear Stage	Amazon	$198.00
Power Supply [1]	DC Power Supply	Amazon	$49.49
3D printer [2]	Creality Ender 3 V2	Amazon	$179.99
Wiring	22 AWG Wire, Solid Core	Amazon	$15.19
Limit Switches	Micro Limit Switches	Amazon	$14.99
3D printer Filament	PLA+ Filament	Amazon	$31.44

[1] While this specific power supply was used, any power supply capable of providing 12V and 2A is sufficient for system operation. [2] Any standard PLA 3D printer is sufficient to print the available STL files; in this study, the Creality Ender 3 V2 Pro model was used.

Operation of the system covers the adhesive removal step of the mechanical exfoliation procedure. Samples are cleaned and prepared using the standard procedure exfoliation until the samples are heat annealed onto the substrate. Samples are then mounted to the angled substrate mounting stage. The system is then homed to a fixed position at the start of each test and the peel angle and speed are defined via a software for speed correction and normalization. Another piece of adhesive tape is attached between the moving stage and the loose end of the tape attached to the substrate. When the start command is issued, the system automatically peels the tape from the substrate at a precisely controlled speed and angle providing a consistent, repeatable peel.

2.3. Software Design

The software is designed to receive serial input commands from a connected computer via standard USB serial monitor software, such as Arduino IDE or VS Code. It uses the Arduino Accelstepper library to control speed and acceleration, and the TMCStepper

library to interface with the motor driver. Although the software is optimized for the Trinamic TMC2209 driver, the libraries are compatible with many other commercially available drivers.

The software provides functions for automatically correcting speed based on the angle of the substrate, as well as for homing the actuator to a fixed position at the start of each test. The source code and related libraries are available on the project GitHub Page, (accessed on 20 January 2025).

2.3.1. Speed Control

The motor speed is controlled using commercially available CNC machine components, powered by an Arduino UNO through a CNC shield expansion board. The CNC shield provides a modular interface for connecting stepper motor drivers to the Arduino using a standardized pin socket. To ensure smooth motion, the motor's step pulses are refined through micro-stepping, which divides each large step into smaller increments for precise, continuous movement.

The system uses a Trinamic TMC2209 stepper motor driver, selected for its quiet operation and high micro-stepping resolution (256 micro-steps), which offers superior precision compared to common alternatives like the Allegro A4988 and Texas Instruments DRV8825. The stepper motor driver controls a NEMA-57 stepper motor, which is connected to a 600 mm linear stage.

The moving stage is equipped with a 3D-printed attachment block to pull the adhesive tape attached to the substrate. The Arduino UNO communicates with a computer via USB cable, receiving serial input for tasks such as starting, stopping, homing, and setting parameters. A separate UART channel interfaces directly with the Trinamic TMC2209 to monitor and adjust motor parameters like position, speed, and micro-steps.

The motor system is powered by a variable DC power supply, while the Arduino is powered through the USB interface. Limit switches are connected to the Arduino to prevent the linear actuator from exceeding its physical limits and to home the actuator to a fixed position at the start of each test. Figure 3 shows the wiring diagram of the system.

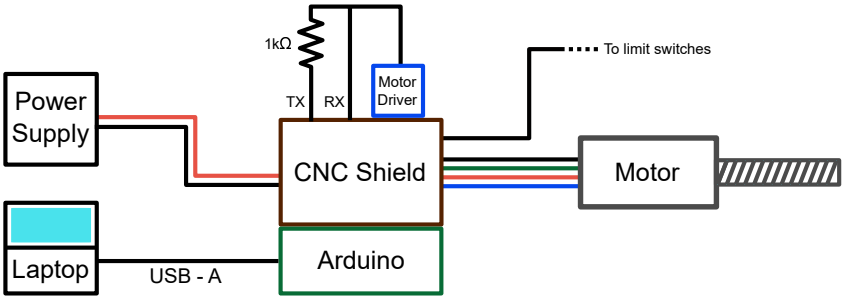

Figure 3. Wiring diagram of the motor control system and interface.

2.3.2. Calculating Peel Speed

Adhesive industry testing has shown that pulling the end of an adhesive strip at a defined rate varies the resultant removal rate on the substrate surface with a different peel angles [19]. For the given system, peeling at 1 mm/s at a 90° will result in a peeling velocity of 1 mm/s; however, pulling the tape at the same 1 mm/s speed at a 180° angle yields a peel speed of just 0.5 mm/s at the substrate surface. To achieve a specific substrate peel velocity, the speed of the horizontal actuator must be adjusted depending on the angle which the sample is positioned. The relationship between the actuator speed and the effective peel speed can be described by Equation (1).

$$\text{Actuator Speed} = \text{Substrate Peel Speed} \times (\cos(\theta) + 1) \quad (1)$$

Equation (2) can be derived from the following equation, which relates the distance the horizontal actuator travels to the distance that has been peeled:

$$h = d(\cos(\theta) + 1) \tag{2}$$

In this context, θ represents the angle between the direction opposite of the pull and the horizontal plane. d represents the distance between the starting and current positions of the peel, and h represents the distance that the horizontal actuator has travelled. $d * \cos(\theta)$ is the horizontal component of the distance peeled, and an additional amount d is added because the distance between the actuator and the peeling location increases by the exact amount of tape peeled.

As the angle is changed between different test runs, the horizontal component of the peel speed varies, necessitating adjustments to the actuator speed each time to maintain a normalized peel rate across tests. When $\theta = 0°$, the sample is pulled horizontally, and the actuator speed is double the peel speed. As θ increases, the horizontal component reduces, requiring a lower actuator speed to achieve the same effective peel speed. This relationship must be considered when normalizing results obtained at different peel angles under fixed speeds. A diagram illustrating the relationship between actuator movement and peel distance is shown in Figure 4b.

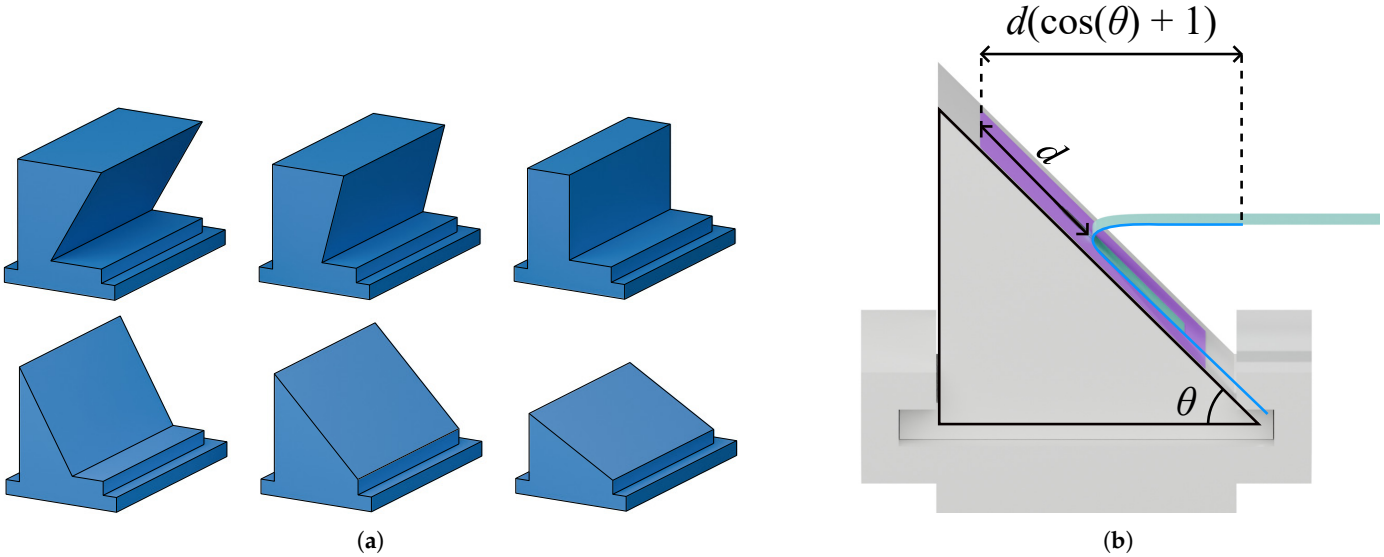

(**a**) (**b**)

Figure 4. Angled substrate mounting blocks and locking base. (**a**) Examples of other modeled substrate mounting blocks, listed from left to right and top to bottom, at 120°, 105°, 90°, 60°, 45°, and 30°. Angles of any incremental degree can be modeled, 3D printed, and interchanged into the system. (**b**) Diagram depicts the correlation between actuator displacement and peel distance, along with an example of a 45° block slotted into the interlocking base. Peel angles are measured from the horizontal plane and are notated as θ.

2.4. Angle Control

The system controls the angle through the use of fixed substrate mounting surfaces with a precise angle relative to the pull direction. The system utilizes interchangeable blocks to be slid horizontally into place via guide rails on a locking base which has been modeled with screw holes to be mounted to an optical table. This rigid design is chosen instead of an adjustable mechanism to prioritize simplicity and to eliminate the potential issues related to improperly secured components and the variability introduced by necessitating tight tolerances in movable parts. The slide-in mount base is designed to raise the height of the substrate to allow for an exact alignment with the axis of the tape pull. As the tape

is peeled from the substrate, a slight difference in height is created between the moving stage and peel height. To compensate for this angle error, the moving stage and substrate mounting stage are placed sufficiently far to keep the change in angle less than 1° over the course of a peel. The graphene samples used for testing are 10 mm, meaning approximately 580 mm or greater distance to keep angle error within the tolerance range. The modular table mounts of the system and 600 mm thread screw length are designed to offer flexibility to allow a similar compensation for larger area samples. Examples of the mounting blocks of different angles are shown in Figure 4a.

3. Results

In Figure 5, the system is shown in a demonstrative test run using a single prepared, clean SiO_2 wafer with multiple samples of tape applied. The bulk crystal used for exfoliation was SPI Supplies Grade-1 HOPG 10 × 10 × 1 mm, with each sample prepared using the same exfoliation process. Samples were exfoliated three times on clean sections of a piece of mother tape then exfoliated a fourth time onto a fresh piece of daughter tape. Deposited flakes were examined using a Horiba Xplora Plus (HORIBA Instruments, Inc., Irvine, CA, USA) video microscope's software mosaic feature to automatically scan high resolution images of sample surface areas. Optical microscopy images of the results, each demonstrated speed and angle combination, are shown in Figure 6. A quick qualitative analysis shows the differences in deposition densities when varying peel angle and speed between a relatively fast pull of 5 mm/s and slow pull of 0.01 mm/s. Images were manually searched for in areas of higher density flakes and were further investigated via optical microscope to determine individual flake surface area and number of layers via Raman spectroscopy, as shown in Figure 7.

The accuracy of speed signals is critical when performing the analysis of very slow peels as an error can compound with each delay cycle of the stepper motor. To properly normalize data compared between different test runs, the speed error of the system must be validated across a wide range to ensure that a similar level of accuracy is achieved in different ranges. Compensation of peel speeds at different angles is also necessary to enable comparison of speed data between runs. The system's accuracy was validated using a stopwatch modified to start and stop based on limit switch inputs placed at a fixed interval on the linear guide rail. The system was measured by the amount of time to travel a fixed distance of 200 mm over several orders of magnitude of speeds. The system demonstrated a relative speed error of less than 0.7% across all tested speeds, ranging from 5 mm/s to 0.001 mm/s. The results of the speed testing are shown in Table 2.

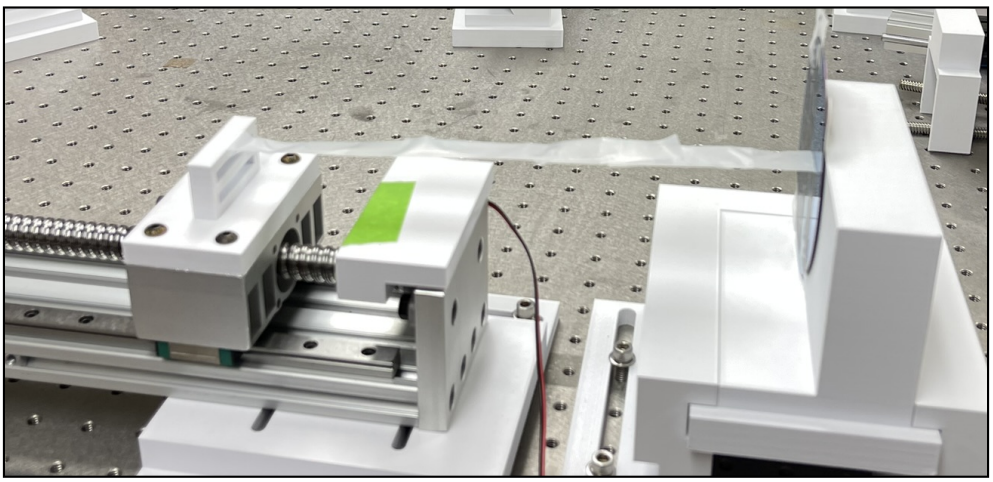

Figure 5. Peeling system in operation with a 90° peel angle.

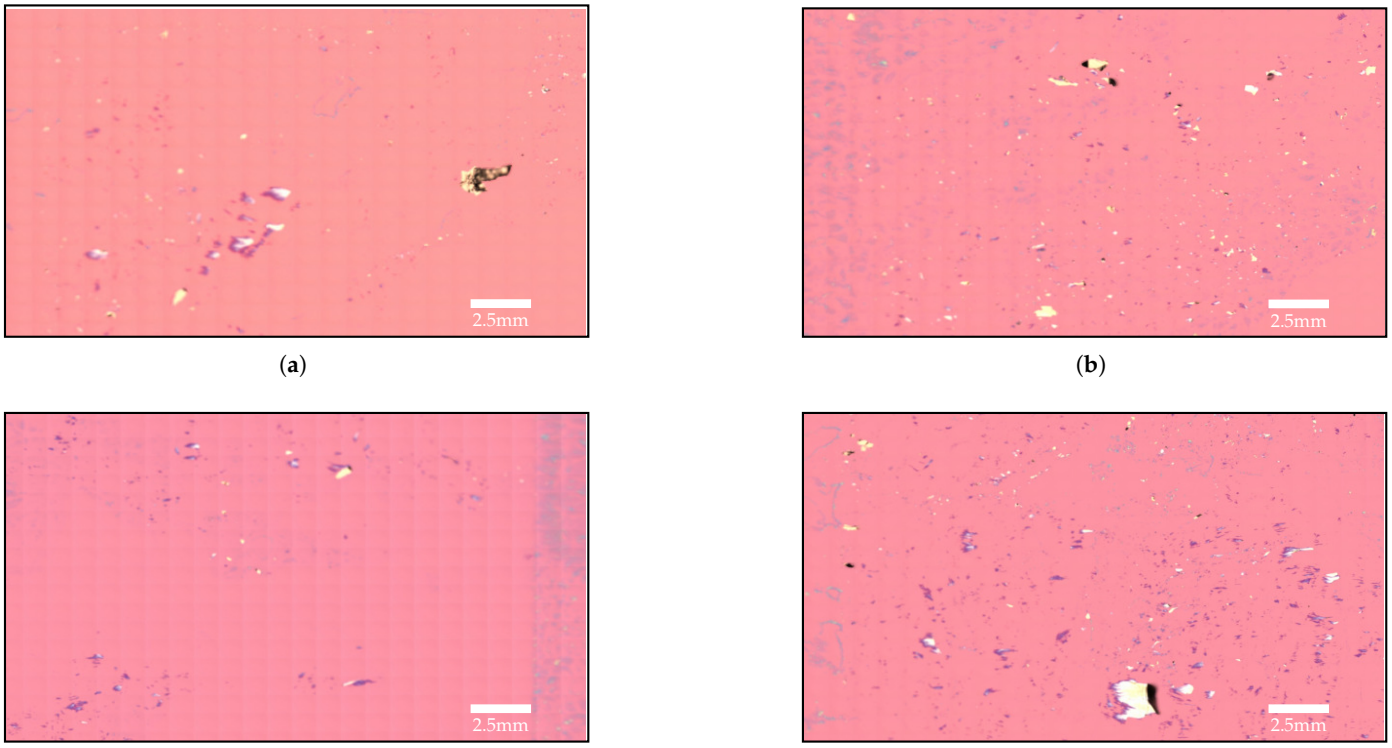

(**a**) (**b**)

(**c**) (**d**)

Figure 6. Differing densities of deposition at different peel angles and speeds. Results of fast 5 mm/s and slow 0.01 mm/s peels at 90° and 180° angles onto a single substrate. Dark blue areas represent few-layer graphene flakes while lighter yellow portions are bulk graphite. Teal areas represent adhesive residue which is often more prominent on slower peels. Image was taken using a mosaic of 50× magnification optical microscopy images.(**a**) Fast pull with 90° peel angle. (**b**) Slow pull with 90° peel angle. (**c**) Fast pull with 180° peel angle. (**d**) Slow pull with 180° peel angle.

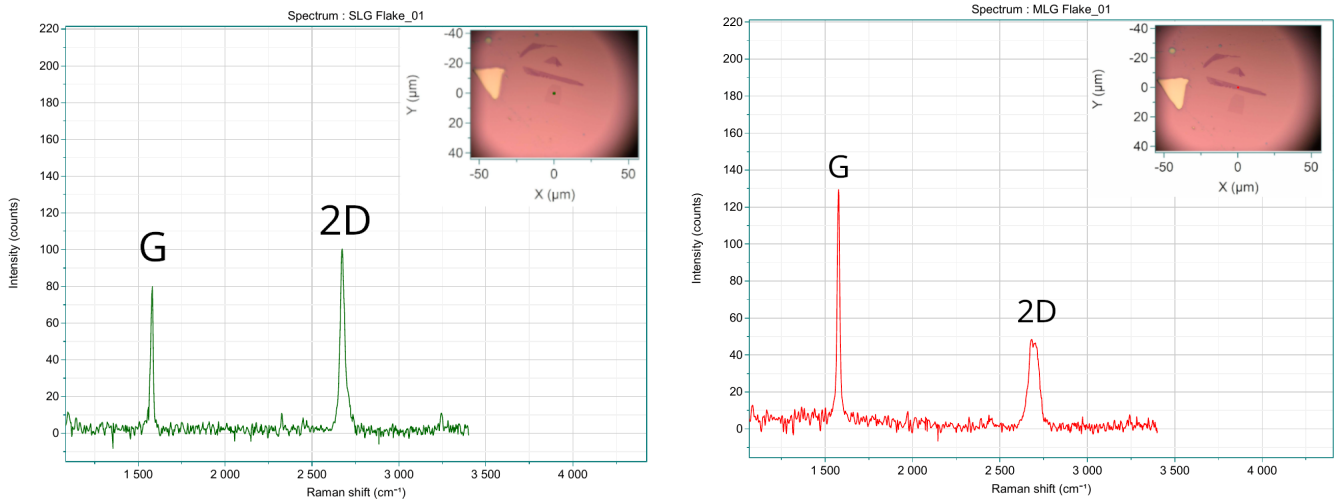

(**a**) (**b**)

Figure 7. Raman spectra evaluation of flakes obtained from the system during a slow 0.01 mm/s peel at a 45° angle. Image and data was taken using a 100× magnification lens on a Horiba Xplora Plus. (**a**) Single-layer graphene (SLG) characterized by a higher intensity 2D peak relative to the G peak. (**b**) Multi-layer graphene (MLG) characterized by the 2D peak intensity higher relative to the G peak; a higher ratio of intensity indicates more layers [16].

Table 2. Results of speed validation testing [1].

Set Speed (mm/s)	Micro Steps [2] (Subdivisions)	Measured Time (s)	Actual Speed (mm/s)	Speed Error (mm/s)	Relative Speed Error (%)
5.00	0	40.12	4.99	0.0150	0.30
1.00	0	199.87	1.00	−0.0007	−0.07
0.50	16	402.59	0.50	0.0032	0.64
0.10	128	2012	0.10	0.0150	0.60
0.01	256	20009	0.01	0.0000	0.04
0.001	256	199813	0.00	0.0000	−0.09

[1] All speeds were tested using a fixed distance of 200 mm. [2] Driver micro steps for speeds <1 mm/s were tested using the highest amount of subdivisions available for a given speed while keeping the stepper motor <1000 steps/s due to Arduino hardware accuracy constraints.

Limitations

The Arduino UNO model is limited at high speeds by its clock frequency, losing accuracy with speeds greater than 10 mm/s. Iterations of this system could incorporate a higher clocked controller; however, theoretical models of adhesive behavior indicate that slower speeds are better suited for the peeling process, suggesting that this limitation is unlikely to pose a concern. Due to RAM constraints on the Arduino UNO, storing strings for relaying text to the end-user interface is limited. This was handled by storing byte string data in flash memory but could also be addressed with a more powerful controller. Another limitation is the slight change in relative peel angle that occurs during a test run due to the point of contact shifting lower as the adhesive is removed from a substrate surface. The worst tested case was ~5.7° over the course of a 30 mm sample using a 300 mm length of tape. This is not a significant concern for the system as the angle variance can be adjusted easily through lengthening distance between the actuator and the substrate before the start of a peel. It was found that a 1 m distance was sufficient to maintain a consistent angle ±1° over the course of a 30 mm peel.

In most cases, slower peel speeds are expected to have larger amounts of residue present; however, the 180° results in Figure 6 could be interpreted to suggest the opposite. This is possibly due to uneven contact with the hotplate during the heat annealing step of the procedure. This specific test was conducted using a single whole 100 mm SiO_2 wafer to normalize the substrate comparison between each sample. During normal procedures, smaller 25 mm × 25 mm wafers are often used instead, which are not expected to have difficulty with even heat distribution.

4. Discussion

This paper presents a bespoke system for enforcing controlled key parameters during the deposition of mechanically exfoliated 2D materials and facilitating optimization through parametric evaluations. The system is designed to be modular and adaptable to a wide range of inexpensive and commercially available linear stages and stepper motors. The example list of components in this publication were produced for less than USD 400 and could easily be disassembled for storage or transportation. This system offers precise, isolated control over peel speed and angle, both of which significantly influence 2D material deposition yields. Tests have verified the system to be accurate within ±0.7% relative speed error over multiple orders of magnitude tested (1 µm to 5000 µm). Furthermore, angle-controlled substrate mounts have been developed, allowing for angle adjustments between 0° and 120°, as shown on the GitHub Page, (accessed on 20 January 2025). The system allows labs and educational institutions to comprehensively examine the most critical

point of the mechanical exfoliation process, and foster an understanding of more optimal conditions that can be created to better scale the production of 2D materials.

Author Contributions: Conceptualization, A.G., R.C.O. and J.A.W.; methodology, A.G.; software, A.G. and Y.-S.D.M.; validation, A.G., Y.-S.D.M., R.C.O. and V.M.L.; formal analysis, A.G.; investigation, A.G.; resources, A.G., R.C.O. and V.M.L.; data curation, A.G.; writing—original draft preparation, A.G. and Y.-S.D.M.; writing—review and editing, A.G., Y.-S.D.M., R.C.O., J.A.W. and V.M.L.; visualization, A.G. and Y.-S.D.M.; supervision, A.G., R.C.O. and V.M.L.; project administration, A.G., R.C.O. and V.M.L.; funding acquisition, A.G. and V.M.L.; All authors have read and agreed to the published version of the manuscript.

Funding: This work was supported and funded by the NAVWAR/NIWC PAC NISE FY24 program.

Institutional Review Board Statement: Not applicable.

Data Availability Statement: Software source code and 3D models available on the GitHub Page (accessed on 20 January 2025). The original contributions presented in this study are included in the article. Further inquiries can be directed to the corresponding author.

Acknowledgments: The authors would like to acknowledge and thank Dave Rees, Joshua MacDermot, and Ryan Lu for sponsoring and managing the NIWC PAC Naval Innovation Science and Engineering (NISE) In-house Innovation Proposal (IIP) program that enabled this research. We would also like to thank the Office of Naval Research (ONR) Veterans to Energy Careers (VTEC) internship program for supporting NIWC PAC intern Yong-Sung Masuda.

Conflicts of Interest: The authors declare no conflicts of interest.

References

1. Novoselov, K.S.; Geim, A.K.; Morozov, S.V.; Jiang, D.; Zhang, Y.; Dubonos, S.V.; Grigorieva, I.V.; Firsov, A.A. Electric Field Effect in Atomically Thin Carbon Films. *Science* **2004**, *306*, 666–669. [CrossRef]
2. Zhao, Q.; Wang, T.; Ryu, Y.K.; Frisenda, R.; Castellanos-Gomez, A. An inexpensive system for the deterministic transfer of 2D materials. *J. Phys. Mater.* **2020**, *3*, 016001. [CrossRef]
3. Cao, Y.; Fatemi, V.; Fang, S.; Watanabe, K.; Taniguchi, T.; Kaxiras, E.; Jarillo-Herrero, P. Unconventional superconductivity in magic-angle graphene superlattices. *Nature* **2018**, *556*, 43–50. [CrossRef]
4. Sulleiro, M.V.; Dominguez-Alfaro, A.; Alegret, N.; Silvestri, A.; Gómez, I.J. 2D Materials towards sensing technology: From fundamentals to applications. *Sens. Bio-Sens. Res.* **2022**, *38*, 100540. : 10.1016/j.sbsr.2022.100540 [CrossRef]
5. Huffstutler, J.D.; Wasala, M.; Richie, J.; Barron, J.; Winchester, A.; Ghosh, S.; Yang, C.; Xu, W.; Song, L.; Kar, S.; et al. High Performance Graphene-Based Electrochemical Double Layer Capacitors Using 1-Butyl-1-methylpyrrolidinium tris (pentafluoroethyl) trifluorophosphate Ionic Liquid as an Electrolyte. *Electronics* **2018**, *7*, 229. [CrossRef]
6. Planillo, J.; Alves, F. Fabrication and Characterization of Micrometer Scale Graphene Structures for Large-Scale Ultra-Thin Electronics. *Electronics* **2022**, *11*, 752. [CrossRef]
7. Huang, Y.; Pan, Y.H.; Yang, R.; Bao, L.H.; Meng, L.; Luo, H.L.; Cai, Y.Q.; Liu, G.D.; Zhao, W.J.; Zhou, Z.; et al. Universal mechanical exfoliation of large-area 2D crystals. *Nat. Commun.* **2020**, *11*, 2453. [CrossRef] [PubMed]
8. Gao, E.; Lin, S.Z.; Qin, Z.; Buehler, M.J.; Feng, X.Q.; Xu, Z. Mechanical exfoliation of two-dimensional materials. *J. Mech. Phys. Solids* **2018**, *115*, 248–262. : 10.1016/j.jmps.2018.03.014 [CrossRef]
9. Ariana Tantillo. Brookhaven National Laboratory. Available online: https://www.bnl.gov/newsroom/news.php?a=217449 accessed on 20 August 2024.
10. Courtney, E.D.S.; Pendharkar, M.; Bittner, N.J.; Sharpe, A.L.; Goldhaber-Gordon, D. Automated Tabletop Exfoliation and Identification of Monolayer Graphene Flakes. *arXiv* **2024**, arXiv:2403.12901.
11. Li, Y.; Kuang, G.; Jiao, Z.; Yao, L.; Duan, R. Recent progress on the mechanical exfoliation of 2D transition metal dichalcogenides. *Mater. Res. Express* **2022**, *9*, 122001. [CrossRef]
12. Polichetti, T.; Miglietta, M.L.; Francia, G. Overview on graphene: Properties, fabrication and applications. *Chim. Oggi* **2010**, *28*, 6–9.
13. Huang, P.; Ruiz-Vargas, C.; Zande, A.; Whitney, W.; Levendorf, M.; Kevek, J.; Garg, S.; Alden, J.; Hustedt, C.; Zhu, Y.; et al. Grains and grain boundaries in single-layer graphene atomic patchwork quilts. *Nature* **2011**, *469*, 389–392. [CrossRef] [PubMed]
14. Liu, N.; Tang, Q.; Huang, B.; Wang, Y. Graphene Synthesis: Method, Exfoliation Mechanism and Large-Scale Production. *Crystals* **2022**, *12*, 25. [CrossRef]

15. Kim, K.; Lee, D.; Chang, C.; Seo, S.; Hu, Y.; Cha, S.; Kim, H.; Shin, J.; Lee, J.-H.; Lee, S.; et al. Non-epitaxial single-crystal 2D material growth by geometric confinement. *Nature* **2023**, *614*, 88–94. [CrossRef]
16. Huang, Y.; Sutter, E.; Shi, N.N.; Zheng, J.; Yang, T.; Englund, D.; Gao, H.J.; Sutter, P. Reliable Exfoliation of Large-Area High-Quality Flakes of Graphene and Other Two-Dimensional Materials. *ACS Nano* **2015**, *9*, 10612–10620. [CrossRef] [PubMed]
17. Islam, M.A.; Serles, P.; Kumral, B.; Demingos, P.G.; Qureshi, T.; Meiyazhagan, A.; Puthirath, A.B.; Abdullah, M.S.B.; Faysal, S.R.; Ajayan, P.M.; et al. Exfoliation mechanisms of 2D materials and their applications. *Appl. Phys. Rev.* **2022**, *9*, 041301. [CrossRef]
18. Davydov, A.; Krylyuk, S.; DiCamillo, K.; Paranjape, M.; Shi, W. Automated Mechanical Exfoliation of MoS2 and MoTe2 Layers for 2D Materials Applications. *IEEE Trans. Nanotechnol.* **2019**, *18*, 144–148.
19. Tsaur, B.; Allen, R. Post-Si Technologies: Emerging Technologies Driving The Future of Semiconductors. Ph.D. Thesis, University of London, London, UK, 2003.